RERTR 2012 — 34th INTERNATIONAL MEETING ON
REDUCED ENRICHMENT FOR RESEARCH AND TEST REACTORS

October 14-17, 2012
Warsaw Marriott Hotel
Warsaw, Poland

Multi-Physics Simulation of the E-FUTURE-1 Fuel Irradiation Experiment

A.M. Tentner, A. Bergeron, Y.S. Kim, G.L. Hofman, J.G. Stevens
GTRI Convert Program, Nuclear Engineering Division
Argonne National Laboratory
9700 S. Cass Ave., Argonne, IL 60439-4803 – USA

S. Van den Berghe
Institute for Nuclear Materials Science, Microstructural and Non-Destructive Analyses
SCK•CEN, Boeretang 200, B-2400 Mol - Belgium

ABSTRACT

A Computational Fluid Dynamics (CFD) model based on the STAR-CD code and a model for the simulation of UMo dispersion Fuel Behavior (FB) are used at Argonne National Laboratory (ANL) for the multi-physics analysis of the E-FUTURE-1 fuel irradiation experiments conducted in the BR2 reactor at SCK•CEN in Belgium. The E-FUTURE experiments are conducted in the framework of the LEONIDAS program in order to qualify UMo LEU fuel for use in the BR2, RHF, and JHR high flux European reactors.

The E-FUTURE-1 experiment irradiated four full sized fuel plates at maximum local heat fluxes of 470 W/cm^2 at Beginning of Life (BOL). Each plate contained dispersed UMo in an Al matrix with a different Si content and/or exposed to a different thermal treatment. The examination of the irradiated fuel plates has yielded valuable data for the model validation. The CFD calculations provide the time dependent cladding and fuel temperatures needed by the fuel behavior code. The occurrence of fuel swelling during irradiation leads to significant changes in the fuel plate geometry and fuel conductivity, which are used by the CFD model to update the fuel temperatures. The integrated multi-physics simulation uses the power generation history to describe the time dependent evolution of the fuel temperature, plate geometry, and fuel composition during the experiment. The models and the model integration strategy are described. Results of recent multi-physics simulations of the E-FUTURE-1 experiment are presented and compared with the measured results of the non-destructive and destructive analyses.

 Work supported by the U.S. Department of Energy, National Nuclear Security Administration's (NNSA's) Office of Defense Nuclear Nonproliferation.

1. Introduction

The effort to develop dispersed UMo LEU fuel elements with densities up to 7.5 - 8.5 gU/cm³ is currently focused on the qualification of LEU fuel elements at high heat-fluxes. The European group LEONIDAS (AREVA-CERCA, CEA, SCK-CEN, ILL) [1] has been formed in 2009 for the qualification of high density LEU fuel based on dispersed UMo for use in the BR2, RHF, and future JHR high flux reactors. In close collaboration with the US GTRI program, Argonne National Laboratory (ANL) and Idaho National Laboratory (INL), the LEONIDAS group has launched an experimental program consisting of irradiation tests and Post-Irradiation Examination (PIE). The high-heat-flux irradiation test named E-FUTURE-1, consisting of 4 full-size flat plates in a dedicated irradiation basket, started in March 2010 and was completed in October 2010 in the BR2 reactor at SCK-CEN. The plates containing dispersed UMo in an Al-Si matrix were irradiated at heat fluxes up to 470 W/cm^2 at BOL. The non-destructive and destructive measurements of the fuel plates provided valuable information about the fuel plate behavior during irradiation which is now being used to guide the development of analytical models. The non-destructive examination of the fuel elements showed significant plate swelling and oxide film formation, and the destructive examination showed substantial changes in the fuel structure, indicative of substantial changes in the fuel conductivities that would lead to increased fuel temperatures. The integrated Computational Fluid Dynamics (CFD) and Fuel Behavior (FB) model [2] developed at ANL with the goal of providing a predictive fuel performance tool was used to simulate the E-FUTURE experiment. Recent developments of the integrated CFD-FB model are described and the experimentally measured changes in the fuel plate dimensions and fuel composition are compared with the corresponding calculated results.

2. The E-FUTURE-1 Experiment

The E-FUTURE-1 irradiation test, designed to allow the selection of the best combination of parameters for the LEU UMo in terms of Si content and thermal treatment, has been completed in the BR2 reactor at SCK-CEN in 2010. It consisted of irradiating four full size flat fuel plates contained in a specially designed basket in the BR2 reactor at high heat fluxes and then in assessing their performance parameters through non-destructive and destructive post-irradiation examinations. The maximum heat flux reached 470 W/cm^2 at BOL, and the maximum ^{235}U burn-up was around 70 %. A schematic cross-section through the fuel basket and cross-sections through the fuel plate are shown in Figures 1 and 2, respectively. The coolant flow enters at the top of the irradiation basket with a nominal temperature of 38 K and flows downward between the fuel plates, exiting at the bottom of the basket. A thicker Al plate installed at the center of the coolant channel, parallel to the fuel plates provides additional rigidity, as shown in Figure 2.

The E-FUTURE plates are full size, high density, flat fuel plates made of dispersed UMo in Al-Si matrix (8 gU/cm^3, 19.7 % ^{235}U enrichment) with two different cladding types (AG3-NET as used in BR2 and AlFeNi as used in RHF). An important parameter specified for the E-FUTURE fuel plate is the Si content in Al matrix required to stabilize the interaction layer formed between the UMo and the Al matrix [3]. Two Si contents (4 and 6 wt%) were chosen for the E-FUTURE test plates. Two different final thermal treatments were also chosen, taking into account US GTRI, CEA and AREVA-CERCA feedback from previous UMo test programs, that had indicated a beneficial influence of the heat treatment on the Si rich layers around the fuel particles formed during fabrication [4]. The fuel parameters chosen for the E-FUTURE fuel plates are summarized in Table 1.

Table 1 E-FUTURE Test Matrix [1]

Plate	Si [%]	Final Heat Treatment	Cladding
U7MC6111	6	2h at 425 C	AlFeNi
U7MC6301	6	4h at 475 C	AG3-NET
U7MC4111	4	2h at 425 C	AlFeNi
U7MC4202	4	2h at 475 C	AG3-NET

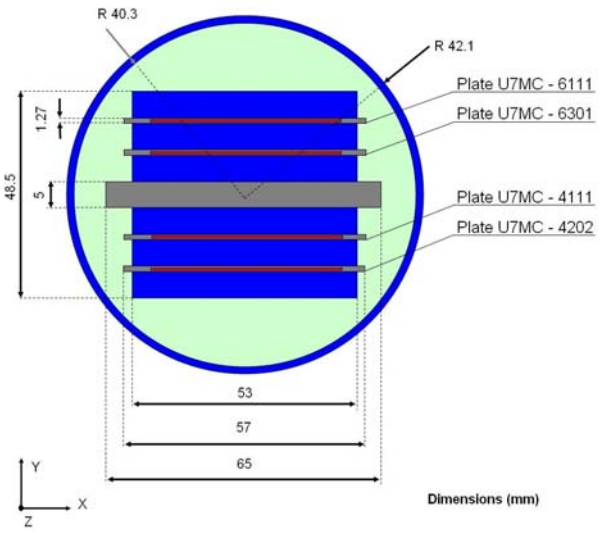

Figure 1 Cross section of the E-FUTURE basket with four U7Mo fuel plates

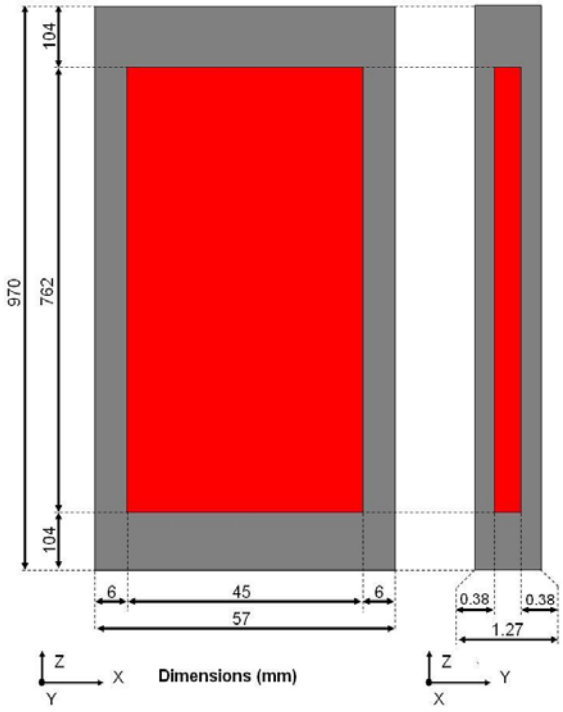

Figure 2 E-FUTURE fuel plate and fuel meat dimensions

3. The Integrated CFD-FB Model of the E-FUTURE-1 Experiment

3.1 The CFD Model

The CFD model, based on the commercial Star-CD code, describes the irradiation basket, containing the four fuel plates and the coolant channels, as illustrated in Figure 3. This figure shows the original geometry of the fuel plates before irradiation. The thickness of the fuel meat and cladding can change during the irradiation, as described in Section 5 below. The coolant enters through an upper plenum at the top of the basket, flows downwards between the fuel plates, and exits at the bottom through a lower plenum. The inclusion of the upper and lower plenum allows the CFD model to calculate the coolant flow redistribution due to any geometrical or thermo-hydraulic differences between the coolant channels. The CFD model includes

conjugate heat transfer, calculating both the thermal-hydraulic conditions of the coolant and the temperatures in the solid fuel plates and basket. The temperature at the outer boundary of the irradiation basket is assumed to be equal to the inlet coolant temperature. The power generation in the fuel plates at a specified time during the irradiation cycle is based on the results of neutronic calculations performed for that time.

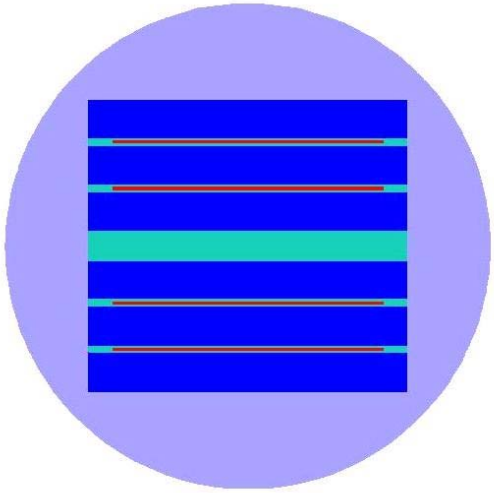

Figure 3 Transversal cross section through the E-FUTURE CFD model showing the fuel plates and coolant channels

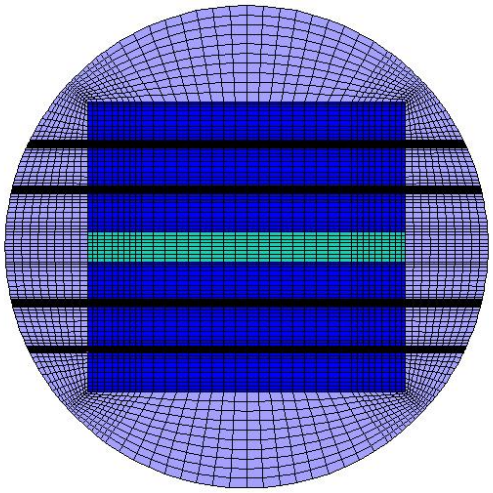

Figure 4 Transversal cross section through the E-FUTURE CFD model showing the computational mesh

This fluid mesh is unequally spaced, with the cell thickness decreasing near the cladding surface, to ensure an adequate y^+ value. A non-uniform mesh has also been used in the fuel meat region, in order to capture the sharp temperature gradients and local temperature peaks that develop in the fuel meat near the boundaries with the non-fuel cladding regions. These temperature gradients are due to the 3-D components of the heat transfer between the fuel and cladding, in the plane of the fuel plate. Previous experience with the RHF CFD analyses [5] - confirmed later by E-FUTURE analyses - has shown that local temperature peaks tend to occur between 3-6 mm from the fuel-cladding boundaries, both along the plate width and along the plate length. In order to accurately calculate these local temperature peaks, five cells with a width of 1 mm have been provided in the fuel meat near the fuel-cladding boundaries. The remaining central section of the fuel meat width is meshed with larger cells with a width of ~2 mm. A similar approach is used for axial meshing of the fuel meat regions, by providing 31 cells with a length of 1 mm at the top and bottom of the fuel meat region. The meshing in a transversal section of the basket and coolant channels is illustrated in Figure 4. The model allows mesh deformations in the direction normal to the fuel plate surface, describing the geometry changes due to fuel plate swelling and oxide formation during irradiation.

3.2 The FB Model

The fuel behavior (FB) model, referred to as SIMDIF (Simulation of Dispersed Fuel), evaluates the changes in the geometry and thermo-mechanical properties of the four full size fuel plates during irradiation. In order to get an accurate spatial solution, we used the same mesh in the fuel region of the plates as the CFD model mesh. The plate faces are also meshed like in the CFD model to model accurately the oxide formation and information exchange between the FB and CFD models at the coolant – cladding interface. SIMDIF describes the sequence of phenomena that occur in the fuel plate during irradiation including: a) oxide layer growth, b) fuel particle swelling, c) interaction layer (IL) growth, d) fission gas generation, e) fuel plate swelling due to fission gas pressure, f) fuel meat porosity changes, and g) fuel meat conductivity changes. Many of these models have been described in [2] and the remaining of this section describes the recent modeling changes implemented in SIMDIF with the goal of providing an enhanced description of the changes that occur during the irradiation in the fuel meat in general, and in the composition and volume of the interaction layer in particular. The importance of these models for an accurate prediction of the fuel plate behavior during irradiation is confirmed by the results of the post-test destructive analysis (see Section 4.2) which indicate that the pillowing of the fuel plates can be directly related to the extent of interaction phase formation.

3.2.1 Fuel Particle Swelling and Consumption

The fuel particle swelling due to irradiation is calculated using a correlation developed at ANL [6] which depends only on the local fission density. This correlation has been built mainly on the numerous irradiation tests of UMo monolithic fuel in which there is no interaction between the fuel and aluminum. In the previous version of SIMDIF [2] it was assumed that the size of the fuel particles - and the swelling of the fuel plate - is determined solely by the fuel particle swelling. This assumption leads to good plate swelling prediction in regions away from the blister region, but over-predicts the fuel particle volume fraction. This effect can be explained by the fact that the diffusion processes that lead to the formation of the interaction or layer consume not only the matrix but the fuel particles as well. This last effect tends to reduce the irradiation-driven swelling of the fuel particles, and must be taken into account when calculating the fuel particle growth during irradiation.

A new model describing the "consumption" of the fuel particles due to the diffusion processes that take place at the fuel particle interface with the IL has then been added to SIMDIF, The total growth of the Interaction Layer (IL) is still calculated during each time step using an empirical correlation developed at ANL. The increase in the interaction layer is divided into two regions, illustrated in Figure 5: a) a fuel region FR at the IL-fuel particle boundary, which leads to the decrease of the fuel particle volume, and b) a matrix region MR at the IL-matrix boundary, which leads to the decrease of the matrix. The fuel and fission gas present if the FR region become part of the interaction layer and the IL fission gas is assumed to be contained in large bubbles, so that the effect of surface tension on the gas pressure can be neglected. This more complex description of the fuel particle swelling and the IL growth lead to improved volume fraction prediction (see Section 5) but tends to reduce slightly the contribution of the fuel particle swelling to the overall plate swelling.

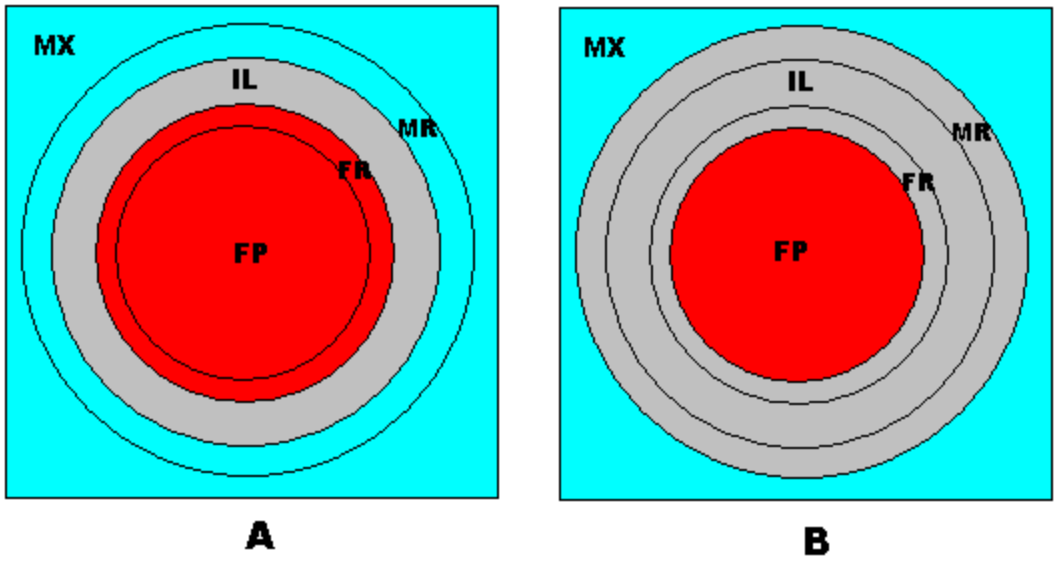

Figure 5 Interaction layer growth: A) IL at the beginning of time step, and B) IL at the end of time step. (grey - interaction layer IL, red - fuel particle FP, blue - matrix MX)

3.2.2 Fission Gas Pressure-Driven Plate Swelling

A new development in SIMDIF is the modeling of the fission pressure driven plate swelling. While in the previous version of SIMDIF [2] it was assumed that the plate swelling is driven primarily by the fuel particle swelling, in the current version of SIMDIF the plate swelling is assumed to be determined by both the fuel particle swelling and the fission-gas-driven pressurization of the cladding. The forces due to these phenomena act simultaneously on the cladding at each mesh location to determine the local plate swelling, as illustrated in Figure 6. While the fuel swelling component of the plate swelling is determined primarily by the local fuel burnup, the plate swelling component due to fission gas pressure is strongly dependent on the local IL region, matrix, and cladding conditions. The IL region separates the fuel particles and the matrix and contains the interaction compounds and the fission-gas-filled pores. The fission gas pressure in the IL region is determined by the amount of fission gas present, local temperature, and available pore volume. The amount of fission gas in the IL region increases during irradiation due to the "consumption" of the fuel particles (see Section 3.2.1) and to the fission of fuel atoms present in the IL. The fission gas present in the IL region is assumed to be contained in large bubbles or pores, so that the effect of surface tension on the gas pressure can be neglected. It is noted that, with this assumption, the actual size or location of the individual pores in the IL region - e.g. pores can accumulate at the IL region boundaries with the fuel or matrix - is not necessary for the fission gas pressure calculation. Coupled with the calculation of porosity volume and local temperature changes, the fission gas content allows the calculation of the local pressure in the IL. This pressure is then used to calculate the local force exerted on the cladding, the associated shear stress in the cladding, and finally a simplified estimate of the expected cladding deformation.

To determine the local plate deformation, SIMDIF assumes that the remaining matrix provides no resistance to swelling and all the resistance to swelling is due to the cladding. A Local Shear Stress (LSS) in the cladding is calculated using the net force difference F_{fg} - F_{fl} exerted on the cladding by the internal force due to the fission gas pressure F_{fg} and the external force due to the coolant fluid pressure F_{fl}. The LSS is compared with an effective yield stress (EYS), calculated as follows:

$$EYS = Ceys * YS(T) \quad (1)$$

Where: YS(T) is the temperature dependent yields stress of the cladding and Ceys is a user selected parameter that accounts for the expected reduction of the YS(T) due to creep and other effects not explicitly considered in this simplified approach. When LSS is greater than EYS local swelling of the plate is allowed until the condition LSS = EYS is satisfied. As the fission gas pressure increases and the cladding resistance decreases this plate swelling component becomes increasingly important and can lead to large local plate deformations.

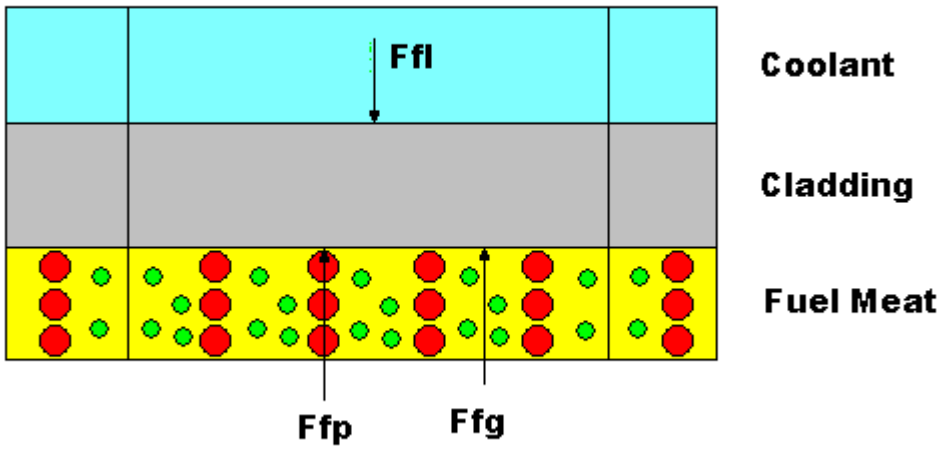

Figure 6 Forces acting on the cladding in the SIMDIF model: a) Fuel particle force Ffp, b) Fission gas force Ffg, and c) Fluid force Ffl (red=fuel particles, green=fission gas filled pores)

3.3 Coupling of the CFD and FB Models

To capture the interactions between the fuel mechanics and thermal-hydraulic effects during the E-FUTURE experiment, each of the three irradiation cycles was divided into two discrete time intervals, resulting in six time intervals as shown in Table 2. It is noted that a coarse time discretization was used to demonstrate the methodology, and finer time intervals can be used in future analyses to increase the accuracy of results.

Table 2 Time intervals for the E-FUTURE experiment simulation

Interval number	Irradiation cycle	Interval limits	Maximum ^{235}U BU [%]
1	310	day 1 (BOC) - day 7	10
2	310	day 8 - day 26 (EOC)	31
3	410	day 1 (BOC) - day 7	39
4	410	day 8 - day 28 (EOC)	55
5	510	day 1 (BOC) - day 10	64
6	510	day 11 - day 20 (EOC)	71

For each time interval, a CFD calculation is performed at the beginning of the interval, using the most current fuel plate geometry, fuel meat conductivity, and oxide layer thickness. An additional CFD calculation is then performed to evaluate the thermal hydraulic conditions at the mid-point of the time interval, using a power generation distribution obtained by averaging the beginning- and end-of-interval power distributions. This mid-interval calculation determines the interval-average fuel meat temperatures and plate-coolant interface temperatures which are then provided to the FB model, as shown in Figure 7. Using this information, the FB model calculates the changes in the fuel conductivity, fuel meat swelling, and cladding oxide growth during the time interval. This information is sent back to the CFD model, which uses the information received from the FB model to change the fuel plate and coolant channel geometry, and then calculates the thermal-hydraulic conditions at the end of the time interval.

The analysis then proceeds to the next time interval, where the procedure described above is repeated. At the beginning of a new irradiation cycle, when the power distribution at the beginning of the time interval is different from that at the end of the previous time interval, a CFD calculation is performed using the plate geometry, fuel conductivity, and oxide thickness available from the end of the previous time interval, but the power distribution corresponding to the beginning of the new time interval. A special procedure was used after the end of the 2nd irradiation cycle 410, to simulate the 180 degree rotation of plate 6111 which was performed during the E-FUTURE experiment. The geometry information provided by the FB model to the CFD model included the changes due to this plate rotation, and the correct geometry of the rotated plate 6111 was used in the CFD calculations during the 3rd cycle 510.

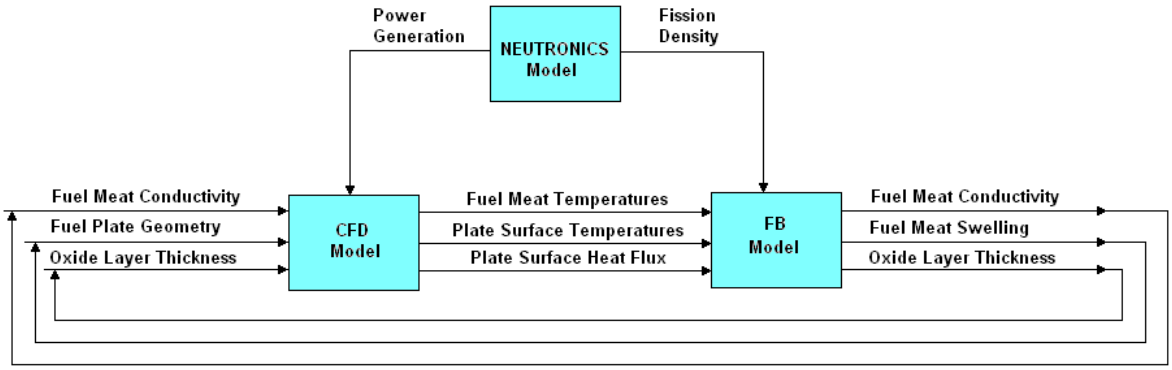

Figure 7 Interactions between the CFD and FB models during E-FUTURE Simulation

4. Post-test Measured Results

4.1 Non-destructive Analysis Results

The non-destructive PIE of the E-FUTURE plates at SCK•CEN with the BONAPARTE measurement bench [7, 8] have revealed the presence of important local swelling in the highest burnup locations of the fuel plates. A marked difference exists in the extent of pillowing between the plates with 4w% Si in their Al matrix and those with 6% Si, with a clearly better behaviour for the latter. Non-destructive analyses included plate thickness and oxide thickness measurements over the complete plate surface. The plate thickness at each point on the plate is corrected for swelling due to the oxide formation on the plate surfaces. If we divide the corrected plate thickness by the initial thickness, the plate swelling is obtained. In order to provide an overview of the axial variation of the plate swelling, the width-average plate swelling is shown in Figures 8 and 9 as a function axial position and burnup, respectively. The width-average plate or oxide thickness is calculated over the plate width at each longitudinal position. It is noted that the plate thickness can vary significantly across the plate width in the blister region. In Section 5 we compare the local measured plate thickness with the corresponding calculated results.

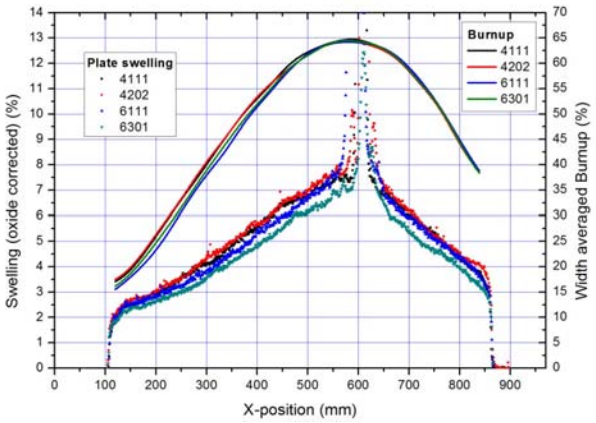

Figure 8 Average plate swelling and average burnup as a function of the axial position

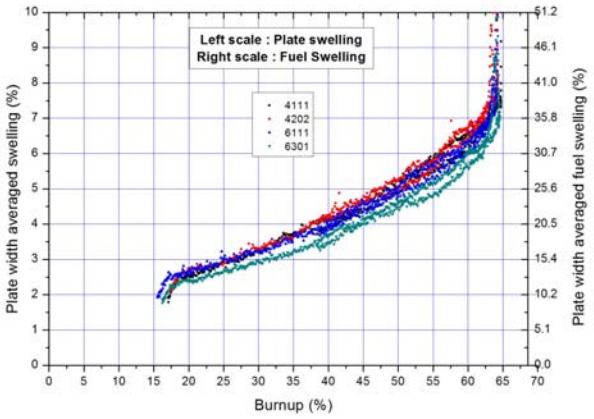

Figure 9 Average plate swelling as a function of burnup

4.2 Destructive Analysis Results

In the destructive examinations, samples were cut from each of the 4 E-FUTURE fuel plates to assess microstructure evolution, particularly interaction layer formation and fission product distribution by microscopy and spectroscopy. The location of the samples is shown in Figure 10. The results were reported in [9]. By Scanning Electron Microscopy, images of the fuel meat were analyzed to determine the volume fractions of Al-Si matrix, interaction phase and fuel kernel. These measured volume fractions can be plotted as a function of burnup, and are compared with the simulation results in Section 5 below. Destructive analyses also allowed verification and validation of the oxide thickness values determined in the non-destructive PIE.

Furthermore, analyses of fission product distribution, particularly Xe, allowed assessing the evolution of the bubble development in the fuel kernels and the interaction product. The main cause for the pillowing of the fuel plates was shown to be directly related to the extent of interaction phase formation. It is noted that recent models added to the SIMDIF fuel behavior model, as outlined in Section 3.2, provide an enhanced description of the changes in the extent and composition of the interaction layer. The destructive analysis results are used to validate and guide further development of these models, as shown in Section 5,

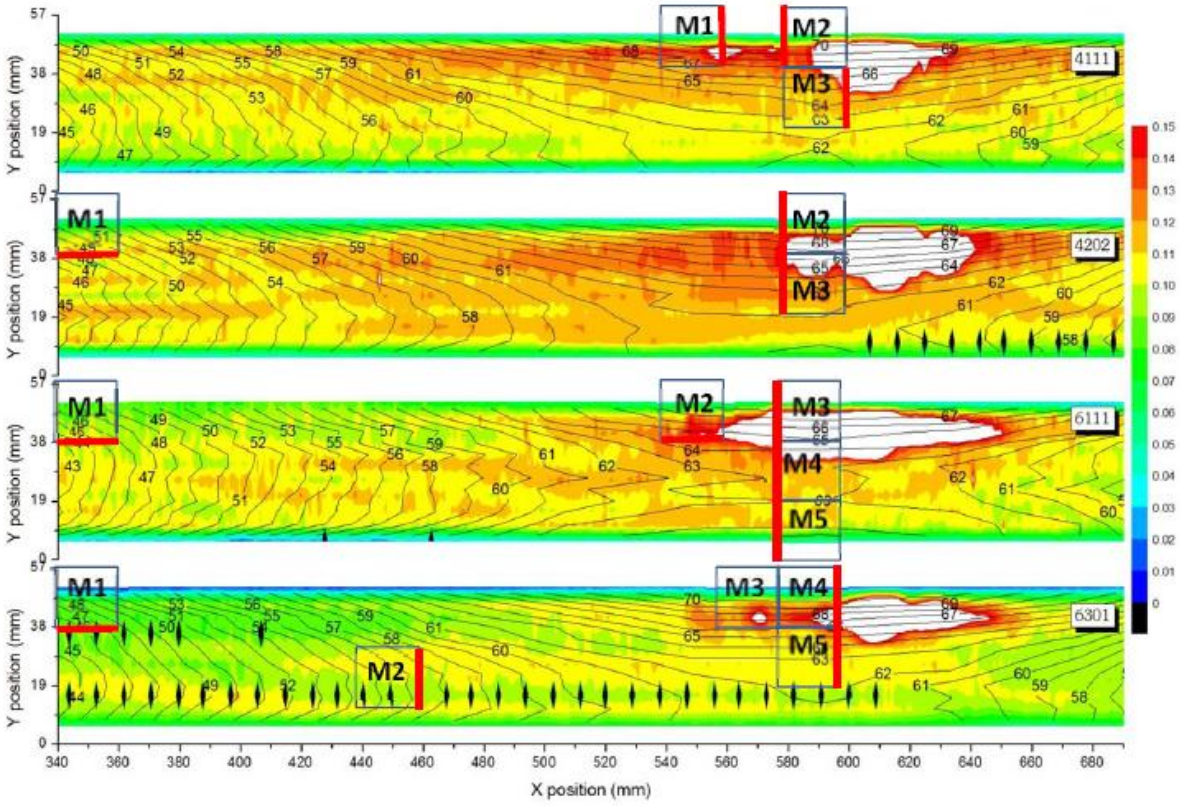

Figure 10 Cutting scheme for the E-FUTURE-1 plates. The color scheme is adapted to show the blistered areas, which have a Swelling-to-Burnup ratio greater than 0.15. The polishing planes are indicated in red [9]

5. Results of Coupled CFD-FB Simulations

Two coupled CFD-FB simulations using different values for the coefficient Ceys - used in equation (1) above - that affects the fuel plate swelling were performed in order to evaluate the effect of this coefficient on the predicted fuel swelling and fuel temperature histories. Both series of calculations simulated the entire E-FUTURE fuel irradiation experiment using the coupled CFD and FB models. In the first simulation series (series A) it was assumed that Ceys = 1.0, i.e. the entire cladding yield stress was used in the plate swelling calculation, without accounting for creep or other effects that could lead to further cladding weakening. This assumption leads to calculated fuel plate swelling values that are ~20% below the measured values in the non-blister regions of the E-FUTURE plates, suggesting that within the framework of the current FB model

the assumed cladding resistance to swelling is too high. There is no indication in this simulation of the much larger deformations observed in the blister regions of the plate. In the second simulation series (series B) it was assumed that Ceys = 0.01, i.e. the effective cladding yield stress was significantly reduced, accounting for creep or other effects that could lead to cladding weakening. This assumption leads to calculated fuel plate swelling values that are close to the measured values in the non-blister regions of the E-FUTURE plates. In a very limited region of the plates, corresponding to the blister region, the calculated swelling remains significantly lower than the swelling observed in the blister regions. A third exploratory simulation (series C) of the E-FUTURE-1 experiment was performed assuming that Ceys = 0.001, i.e. the effective cladding yield stress was further reduced from the value used in series B. This assumption leads to calculated fuel plate swelling values that are significantly higher in the blister regions of the plate, approaching the observed swelling values in some cases. These higher calculated swelling values, however, extend over larger regions of the plates than the observed blister regions, and the agreement between the calculated and observed values in the off-blister regions is generally degraded. In this section we present the results of series B simulations, which currently provide the best agreement with the experimental plate swelling values. It is noted that the change of the coefficient Ceys, which affects directly the plate swelling results, has little effect on the fuel plate composition results presented below.

The coupled CFD-FB calculations sequentially analyzed the time intervals shown in Table 2, using the CFD-FB data transfer procedure described in Section 3.3. The fuel meat and cladding surface temperatures are both affected by the change in the total and local power generated in the fuel meat during irradiation. The fuel meat thickness and conductivity, as well as the cladding-surface oxide layer thickness change during each time step leading to changes in the fuel meat temperatures. The history of the total power generated in the fuel plates 6301 and 4111 is shown in Figure 11. The maximum cladding surface temperature history for the same plates is shown in Figure 12.

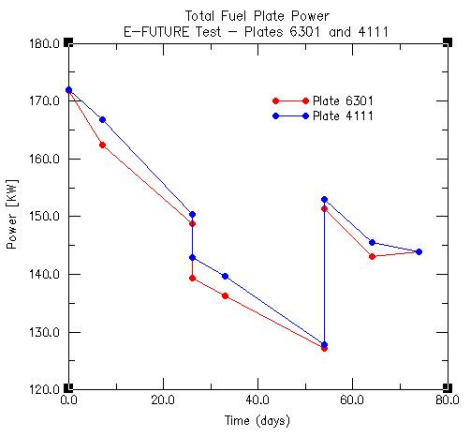

Figure 11 Power generation histories for fuel plates 4111 and 6301

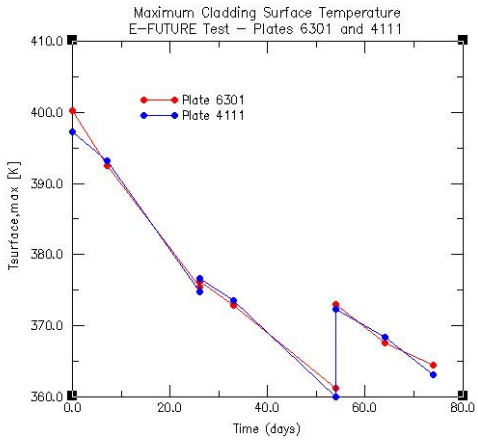

Figure 12 Maximum cladding surface temperature history for fuel plates 4111 and 6301

.

The histories of the maximum fuel temperature calculated for the fuel plates 6301 and 4111 are shown in Figure 13. The maximum fuel temperature increases significantly during the irradiation, even when the power generated in the fuel meat decreases, due to the increasing thermal resistance of the fuel plate. The maximum fuel temperatures calculated for plate 4111 are higher than those of plate 6301 by 15.4 K at the end of the irradiation experiment and by 11.3 K at the beginning of the third irradiation cycle when the highest temperature during the irradiation occurs. The fuel temperature history exhibits a highly non-linear behavior indicating the need for coupling the thermal-hydraulic and fuel mechanics models in the E-FUTURE experiment analysis.

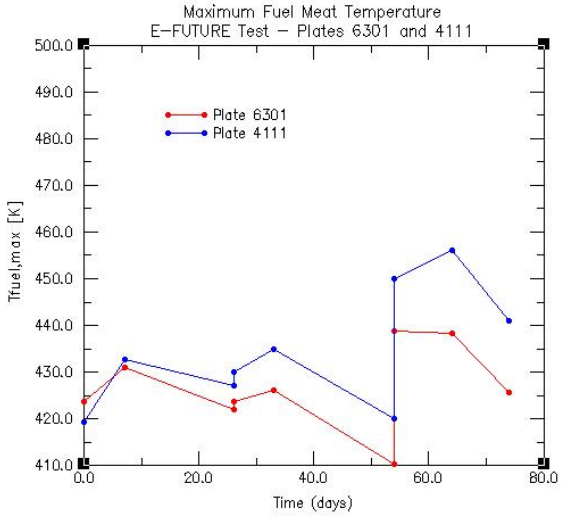

Figure 13 Maximum fuel meat temperature history (plates 4111 and 6301)

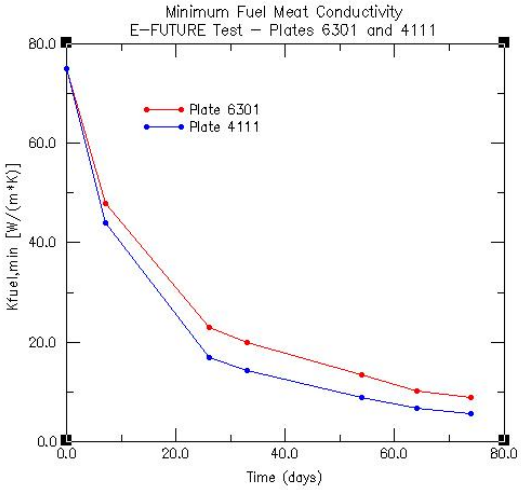

Figure 14 Minimum fuel meat conductivity history (plates 4111 and 6301)

The increase of the plate thermal resistance is due to the decreasing fuel conductivity, fuel meat swelling, and increasing oxide layer thickness, effects which are calculated by the fuel mechanics models. The histories of the minimum fuel meat conductivity for plates 6301 and 4111 calculated are shown in Figure 14. The fuel conductivity decreases rapidly during the first two irradiation cycles, and continues to decrease reaching a minimum value of ~9 W/(m*K) for plate 6301 and ~6 W/(m*K) for plate 4111 at the end of the simulation. The fuel meat conductivity is determined by the fuel meat composition, which changes continuously during the irradiation. The volume fractions of the fuel, interaction layer, and matrix at the end of the experiment were measured at several locations during the destructive examination, as described above in section 4.2. A comparison of the calculated volume fractions for with the corresponding measured values is presented for the plates 4202 and 6301 in Figures 15 through 17, respectively.

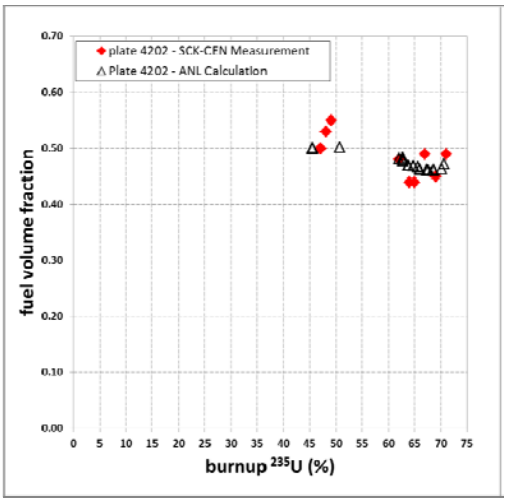

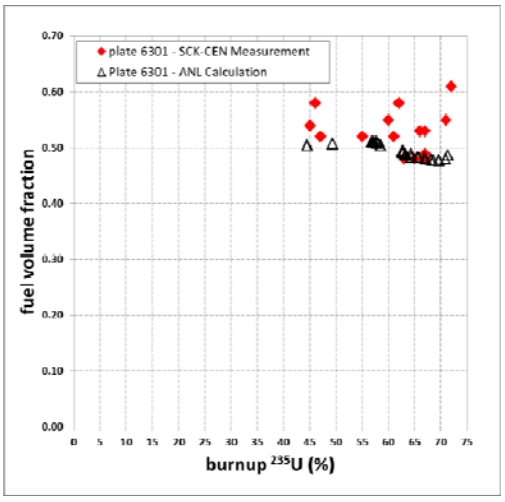

Figure 15 Fuel volume fraction versus burnup: a) plate 4202 left, b) plate 6301 right

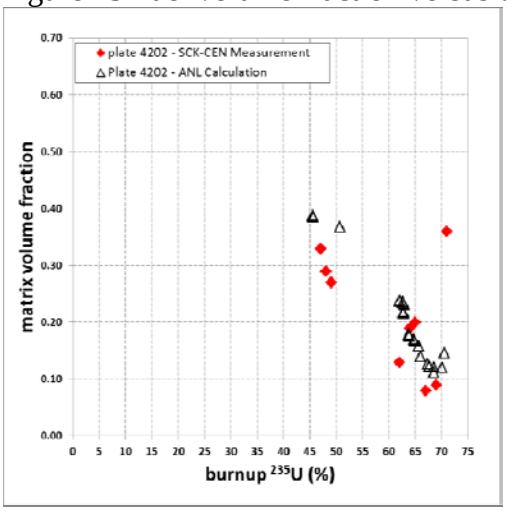

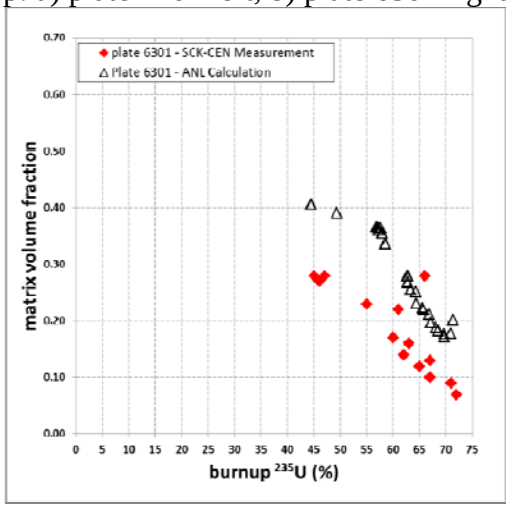

Figure 16 Matrix volume fraction versus burnup: a) plate 4202 left, b) plate 6301 right

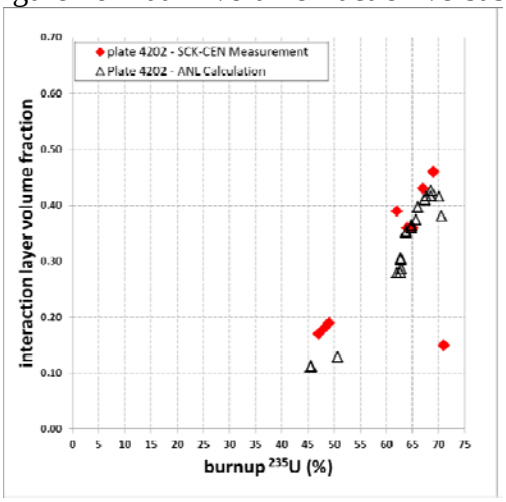

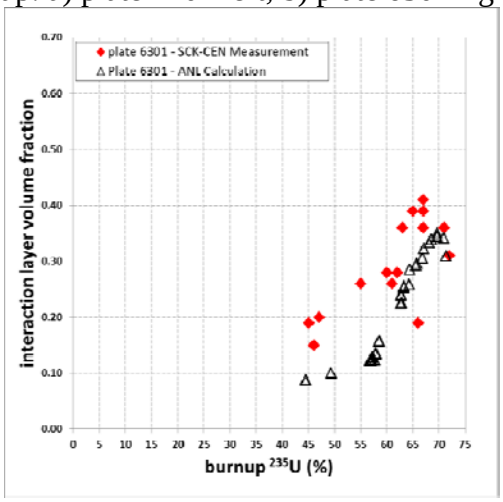

Figure 17 Interaction Layer volume fraction versus burnup: a) plate 4202 left, b) plate 6301 right

The simulation results shown in Figures 15 through 17 show the calculated swelling at selected locations that correspond to the destructive analysis plate cuts used to obtain the corresponding experimental results. These plate cuts are shown in Figure 10 above. Good agreement is obtained for all the four plates, indicating that the SIMDIF model describes fairly well the dominant phenomena that influence the fuel composition changes during irradiation. Reasonably good agreement is also observed when comparing the calculate weight fractions of UMo, Al, and Si present in the interaction layer at specific locations with the corresponding measured values, as shown in Table 3.

The fuel meat temperature and cladding thickness are both influenced by the thickness of the oxide film formed on the cladding surface. The oxide thickness predicted by the FB model at 10 mm from the high power edge for plates 4111 and 6301 is compared with the corresponding measured values in Figure 18. The predicted oxide thickness is significantly lower than the measured values in the blister region, and is somewhat higher than the measured values away from the blister region. This behavior is typical for all the plates, although the magnitude of the peak is different at various distances from the high power edge of the plate. Future work is planned to determine the cause for and reconcile these differences between the predicted and measured oxide thickness values.

Table 3 Weight fraction of UMo, Al, and Si in the IL

		UMo [wt%]		Al [wt%]		Si [wt%]	
Plate	Sample	Measured	Model	Measured	Model	Measured	Model
6301	M2	55.9	56.1	41.7	34.5	1.9	2.2
4202	M3	65.1	53.6	25.6	37.2	2.6	1.6
6111	M4	63.6	54.2	31.7	35.8	0.7	2.3
6302	M5	62.7	54.0	25.9	34.5	2.2	2.3

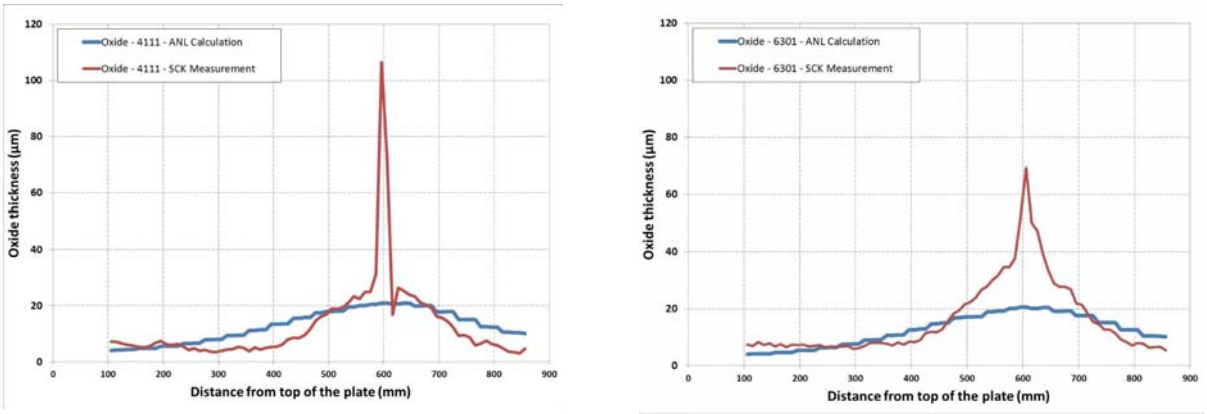

Figure 18 Oxide fuel thickness versus distance from top of the plate, at 10 mm from the high power edge, for plates 4111 (left) and 6301 (right)

The calculated fuel plate swelling for plates 4111 and 6301, at 10 mm from the high power edge, is compared with the corresponding measured swelling in Figure 19. Good agreement between the calculated and measured swelling is obtained over most of the plate, with the exception of a narrow region at the blister location. The same trend is observed for all the fuel plates at various distances from the high power edge of the plate.

It is reminded that the plate swelling results presented above were obtained with a constant value of the coefficient defined in Equation (1) Ceys = 0.01. Additional exploratory calculations performed with a lower value Ceys = 0.001 yield higher cladding swelling values, which approach in some cases the values observed experimentally in the blister region. Future work will focus on implementing a more accurate modeling of the cladding yield stress characteristics that could further improve the SIMDIF prediction of the fuel plate swelling in the blister region.

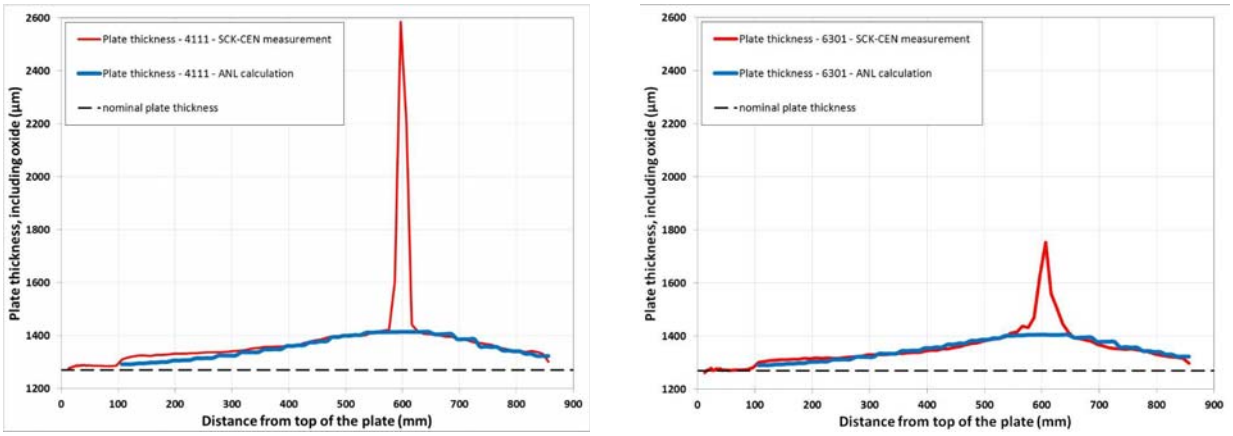

Figure 19 Fuel plate thickness versus distance from top of the plate, at 10 mm from the high power edge, for plates 4111 (left) and 6301 (right)

6. Conclusions

A multi-physics model, including integrated CFD and FB modules has been developed for the analysis of the E-FUTURE-1 fuel irradiation experiment conducted in the BR2 reactor at SCK-CEN in Belgium. The CFD calculations provide the time dependent 3-dimensional fluid and solid temperature distributions and the surface heat transfer information needed by the FB model, which calculates and returns to the CFD model the fuel meat swelling, fuel conductivity and oxide layer changes. The CFD model modifies the computational mesh to reflect the plate geometry changes and uses the modified mesh, fuel meat conductivity, and oxide thickness in subsequent calculations.

In order to better understand and predict the pillowing of fuel plates recent additions to the SIMDIF fuel behavior module include enhanced models describing the changes that occur in the interaction layer and the fuel particles during irradiation and a model that describes the fission-gas pressure-driven swelling of the fuel plate, in addition to the swelling due to fuel particle swelling. Results of the multi-physics simulations of the E-FUTURE-1 using the new SIMDIF models were compared with the experimental results obtained from the post-test destructive and non-destructive analyses. The calculated volume fractions of fuel, interaction layer, and matrix are shown to be in good agreement with the measured results for all the fuel plates. Reasonable

agreement is also obtained between the calculated and measured weight fractions of the IL components. Some differences between the calculated and measured oxide layer are noted, particularly in the area surrounding the blisters. The source of these differences will be examined in future work. Good agreement between the calculated and measured fuel plate swelling is obtained for all plates, with the exception of a narrow region in the neighborhood of the blister. Future work will focus on refining the current simple model describing the weakening of the cladding and subsequent pressure-driven swelling with the goal of improving the plate swelling prediction in the blister region of the plates.

The multi-physics CFD-FB methodology developed includes a clearly-defined interface between the CFD and the FB modules, providing a flexible framework for the evaluation of other FB models. Coupling of the CFD model with other fuel mechanics code such as DART [10] will be explored in future work.

7. References

[1] F. Frery et al., “LEONIDAS U(Mo) Dispersion Fuel Qualification Program: Progress and Prospects,” Proceedings of the 32nd International Meeting on Reduced Enrichment for Research and Test Reactors, Lisbon, Portugal, October 10-14, 2010.

[2] A.M. Tentner, A. Bergeron, Y.S. Kim, G.L. Hofman, J.G. Stevens, "An Integrated Computational Fluid Dynamics and Fuel Mechanics Model for the Analysis of the E-FUTURE Fuel Irradiation Experiment", Proceedings of the 33rd International Meeting on Reduced Enrichment for Research and Test Reactors, Santiago, Chile, October 23-27, 2011.

[3] G.L. Hofman, Y.S. Kim, "Utilizing the stabilizing effect of silicon in U-Mo/Al dispersion and minimum Si addition for the BR-2 test", Intra-laboratory ANL Memo, Aug 11, 2009.

[4] D.D. Keiser, A.B. Robinson, D.E. Janney and J.F. Jue, "Results of recent microstructural characterization of irradiated U-Mo dispersion fuels with Al alloy matrices that contain Si", Proceedings of RRFM-2008, Hamburg, Germany, March 2-5 2008.

[5] A. Tentner, F. Thomas, A. Bergeron, and J. Stevens, "Thermal-Hydraulic Safety Analyses for conversion of the Laue Langevin Institute (ILL) High Flux Reactor (RHF) form HEU to LEU Fuel," Proceedings of the 32nd International Meeting on Reduced Enrichment for Research and Test Reactors, Lisbon, Portugal, October 10-14, 2010.

[6] Y.S. Kim, G.L. Hofman, "Fission product induced swelling of U-Mo alloy fuel", Journal of Nuclear Materials 419, 2011.

[7] S. Van den Berghe, Y. Parthoens, F. Charollais, Y. S. Kim, A. Leenaers, E. Koonen, V. Kuzminov, P. Lemoine, C. Jarousse, H. Guyon, D. Wachs, D. Keiser Jr, A. Robinson, J. Stevens and G. Hofman, Journal Of Nuclear Materials 430 (1-3), 2012.

[8] S. Van den Berghe, A. Leenaers and Y. Parthoens in: Proceedings of the International Meeting On Reduced Enrichment For Research And Test Reactors (RERTR), Santiago, Chile, October 2011.

[9] A. Leenaers, J. Van Eyken, S. Van den Berghe, E. Koonen, F. Charollais, P. Lemoine, Y. Calzavara, H. Guyon, C. Jarousse, B. Stepnik, D. Wachs and A. Robinson in: Proceedings of the International Conference on Research Reactor Fuel Management (RRFM), Prague, Czech Republic, October 2012.

[10] J. Rest, "The DART Dispersion Analysis Research Tool: A Mechanistic Model for Predicting Fission-Product-Induced Swelling of Aluminum Dispersion Fuels", ANL report ANL-95/36, Argonne, Illinois, August 1995